



Identifying NO_x Sources in Arequipa, Peru Using Nitrogen Isotopes in Particulate Nitrate

Greg Michalski^{1*}, Adriana E. Larrea Valdivia², Elizabeth Olson¹, Lisa Welp¹, Huan Fang¹, Kento Magara-Gomez³, Lino Morales Paredes², Juan Reyes Larico² and Jianghanyang Li¹

¹Purdue University, West Lafayette, IN, United States, ²National University of Saint Augustine, Arequipa, Peru, ³Universidad Pontificia Bolivariana-Bucaramanga, Bucaramanga, Colombia

OPEN ACCESS

Edited by:

David Widory,
Université du Québec à Montréal,
Canada

Reviewed by:

Sanjeev Dasari,
UMR5001 Institut des Géosciences
de l'Environnement (IGE), France
Zhiyuan Cong,
Institute of Tibetan Plateau Research
(CAS), China
Yunting Fang,
Institute of Applied Ecology (CAS),
China

*Correspondence:

Greg Michalski
gmichals@purdue.edu

Specialty section:

This article was submitted to
Toxicology, Pollution and the
Environment,
a section of the journal
Frontiers in Environmental Science

Received: 09 April 2022

Accepted: 26 May 2022

Published: 28 June 2022

Citation:

Michalski G, E. Larrea Valdivia A,
Olson E, Welp L, Fang H,
Magara-Gomez K, Morales Paredes L,
Reyes Larico J and Li J (2022)
Identifying NO_x Sources in Arequipa,
Peru Using Nitrogen Isotopes in
Particulate Nitrate.
Front. Environ. Sci. 10:916738.
doi: 10.3389/fenvs.2022.916738

We reported on the first time series of $\delta^{15}\text{N}$ in aerosol nitrate from South America. Particulate matter less than 2.5 microns in diameter ($\text{PM}_{2.5}$) was collected at four sites located in Arequipa, a major city in southern Peru. The $\delta^{15}\text{N}$ values for nitrate in $\text{PM}_{2.5}$ ranged from -1.7 – 15.9% and averaged $5.3 \pm 3.0\%$, with no significant difference between the four study sites and no discernable seasonal trend. These values are significantly higher than those in aerosol nitrate from southern hemisphere marine environments and those from the northern hemisphere. We explain the elevated values using an isotope mass balance mixing model that estimates a source NO_x $\delta^{15}\text{N}$ of $-8 \pm 3\%$, derived mainly from anthropogenic sources (vehicles, industry). An isotope enabled 0-D photochemical box model was used to estimate the isotope enrichment of nitrate relative to NO_x due to kinetic, equilibrium, and photolysis isotope effects occurring during NO_x oxidation. This “source plus photochemistry” approach resulted in general agreement with the observations. This suggests that if the photochemistry effect can be accounted for, nitrate $\delta^{15}\text{N}$ can be used to assess the relative importance of NO_x sources and could be a new tool to validate NO_x emission inventories.

Keywords: isotope N 15, aerosol, Peru, NO_x —oxides of nitrogen, air quality (AirQ)

INTRODUCTION

Air quality is important because it impacts human quality of life and health, yet relative to northern hemisphere countries, there are relatively few studies that have investigated air quality in developing countries in South America, particularly Peru (Pearce et al., 2009; De La Cruz et al., 2019; Alvarez-Tolentino & Suarez-Salas, 2020; Romero, et al., 2020). According to the World Health Organization (WHO) air pollution is a leading cause of global mortality, accounting for an estimated seven million premature deaths (Lelieveld et al., 2015). Roughly 3.7 million of these deaths are partially attributed to outdoor air pollution within cities and these disproportionately impact disadvantaged populations (Hajat et al., 2015). Aerosols and some trace gases, such as nitrogen oxides ($\text{NO}_x = \text{NO} + \text{NO}_2$), SO_2 , and O_3 are the main vectors for the adverse effects of poor air quality. Of the few studies that have been published on Peruvian air quality, most have focused on Lima, Peru’s capital city (Silva et al., 2017; Romero, et al., 2020; Romero, et al., 2020). Like many large cities in developing countries, Lima suffers from poor air quality that is associated with vehicle traffic, industry, and commerce (Romero, et al., 2020; Romero, et al., 2020). There are only a couple of published air quality studies in Peru outside of Lima (Pearce et al., 2009; De La Cruz et al., 2019; Alvarez-Tolentino & Suarez-Salas, 2020) and only recently has one been published on air quality in Arequipa, Peru’s second largest city

(Valdivia et al., 2020; Olson et al., 2021). Despite their importance, ground based air quality studies of aerosols, trace gases, and other air pollutants in Arequipa are noticeably absent.

One of the main compounds found in aerosols produced in large cities such as Arequipa is atmospheric nitrate ($\text{NO}_{3\text{atm}}^-$), a secondary pollutant that plays a key role in atmospheric chemistry. $\text{NO}_{3\text{atm}}^-$ is the sum of nitrate ions dissolved in rain, fog, or clouds ($\text{NO}_{3\text{(aq)}}^-$), gas phase nitric acid produced photochemically ($\text{HNO}_{3\text{(g)}}$), and particulate nitrate (pNO_3^-) produced by N_2O_5 heterogeneous reactions or by uptake of HNO_3 on existing aerosols surfaces (Monks, 2005; Monks et al., 2009). $\text{NO}_{3\text{atm}}^-$ is the reaction product of NO_x , which is mainly emitted by combustion, that is then oxidized via O_3 and organic radical chemistry (Seinfeld & Pandis, 1998; Pye et al., 2010) into higher nitrogen oxides ($\text{NO}_y = \text{NO}_x + \text{NO}_{3\text{atm}}^- + \text{all other N oxides}$). NO_x and $\text{NO}_{3\text{atm}}^-$ are key components of atmospheric chemistry (Monks et al., 2009), controlling the oxidation state of the troposphere (Prinn, 2003), influencing particulate matter (PM) formation (Feng & Penner, 2007), altering the pH of rainwater (Lynch et al., 2000), and facilitating the movement of nitrogen through the N cycle (Galloway et al., 2003). NO_x also produces ozone (O_3) either directly through NO_2 photolysis, or indirectly as a catalyst when volatile organic compounds (VOCs) are present (Monks, 2005). O_3 photolysis, in turn, generates OH radicals that initiates a radical chain reaction involving HO_2 and organic peroxide propagators that results in the oxidation of chemically reduced compounds and the formation of secondary PM (Seinfeld & Pandis, 1998; Finlayson-Pitts & Pitts, 2000) including nitrate and sulfate aerosols (Pusede et al., 2016; Cao et al., 2017; Pan et al., 2018). Thus, understanding NO_x sources and the photochemistry that converts it into $\text{NO}_{3\text{atm}}^-$ is critical for understanding the origin poor air quality.

Despite this importance, there are numerous knowledge gaps in understanding the cycling of NO_y in the atmosphere, particularly in South America. The NO_x emission budget is still poorly constrained. Most emission inventories rely on fixed emission factors for some sources that may, in fact, be spatially or temporally variable. For example, power plant NO_x emissions are based on assumed efficiency of catalytic converters that may not be accurate in all operating conditions (Srivastava et al., 2005; Felix et al., 2012). Soil NO emissions are highly dependent on soil moisture, redox conditions, fertilizer application rates, type, and timing making them challenging to constrain (Galloway et al., 2004; Pilegaard, 2013). There are also several unresolved issues regarding the chemistry that transforms NO_x into $\text{NO}_{3\text{atm}}^-$. These include uncertainties in heterogeneous uptake coefficients of N_2O_5 (Brown et al., 2001; Brown et al., 2006; Chang et al., 2011), the formation of organic nitrates in urban forests (Kastler & Ballschmiter, 1998; Romer et al., 2016), the relative importance and mechanism of HONO formation versus HONO emissions, and reactions of NO_y in the aqueous phase and mixed aerosols (Zhang et al., 2019; Guo et al., 2020; Peng et al., 2020). Further, chemical transport models (CTMs) do not accurately predict aerosol nitrate concentrations or other NO_y mixing ratios (Spak & Holloway, 2009; Y.; Zhang et al., 2009) making predicting $\text{NO}_{3\text{atm}}^-$ formation a significant challenge.

Therefore, it is important that these uncertainties in NO_y cycling be resolved if we aim to have accurate air quality forecasts used to try an develop quality mitigation strategies aimed at improving poor air.

It has been suggested that stable N isotopes can provide clues to the origin of NO_x (Elliott et al., 2009; Felix & Elliott, 2014; Walters, Tharp, et al., 2015) and the oxidation pathways that transform into nitrate (Walters & Michalski, 2015, 2016). $\delta^{15}\text{N}$ is defined by the relative difference between the $^{15}\text{N}/^{14}\text{N}$ ratio in a N compound and the ratio in air N_2 (the arbitrary reference compound) and is typically reported in delta notation (in permil, ‰):

$$\delta^{15}\text{N}(\text{‰}) = \left(\frac{(^{15}\text{N}/^{14}\text{N})_{\text{sample}}}{(^{15}\text{N}/^{14}\text{N})_{\text{airN}_2}} \right) * 1000 \quad (1)$$

Isotopic measurements of $\text{NO}_{3\text{atm}}^-$ show a wide range of $\delta^{15}\text{N}$ values, which has been suggested to indicate variability in NO_x emission sources, chemical processing, and/or a combination of these effects. A number of studies have measured the $\delta^{15}\text{N}$ values of NO_x collected from NO_x sources such as power plants (Felix et al., 2012), automobiles (Walters, Goodwin, et al., 2015), biomass burning (Fibiger & Hastings, 2016), and non-road sources (Felix & Elliott, 2014). Many studies have measured the $\delta^{15}\text{N}$ values of $\text{NO}_{3\text{atm}}^-$ collected from the troposphere. Most of the $\text{NO}_{3\text{atm}}^-$ $\delta^{15}\text{N}$ data is for nitrate that has been collected on filters ($\text{PM}_{2.5}$, PM_{10} , TSP (total suspended particles)) (Moore, 1977; Savard et al., 2017), as the dissolved NO_3^- anion in rain (Heaton, 1987; Hastings et al., 2003; Elliott et al., 2007; Felix et al., 2015), or as gas phase HNO_3 (Elliott et al., 2009; Savard et al., 2017). The range of $\text{NO}_{3\text{atm}}^-$ $\delta^{15}\text{N}$ values span from -50 to +15‰ but the average is ~0‰ (Song et al., 2021).

Two hypotheses have been offered to explain these variations: source and photochemistry. The source hypothesis (Elliott et al., 2007; Hastings et al., 2013) suggests that the $\text{NO}_{3\text{atm}}^-$ $\delta^{15}\text{N}$ range reflects the spatial and temporal mixing of NO_x sources with different $\delta^{15}\text{N}$ values that is then converted into $\text{NO}_{3\text{atm}}^-$. The photochemistry hypothesis (Freyer, 1978; Freyer et al., 1993; Walters et al., 2018) suggests that the observed $\text{NO}_{3\text{atm}}^-$ $\delta^{15}\text{N}$ variations arise via isotope effects occurring when photochemical cycling partitions N into the myriad of NO_y compounds. Recent modeling work (Fang et al., 2021), has shown that only a handful of reactions in the NO_y cycle impact the $\delta^{15}\text{N}$ of nitrate. These include NO_2 photolysis (photo induced isotope effect; Miller and Yung, 2000), the kinetic isotope effect occurring during the $\text{NO} + \text{O}_3$ reaction (Walters and Michalski, 2016), equilibrium isotope effect during the $\text{NO}_2 + \text{OH}$ (Fang et al., 2021) and $\text{NO}_2 + \text{NO}_3 \leftrightarrow \text{N}_2\text{O}_5$ (Walters and Michalski, 2015) reactions, and isotope exchange reaction $^{15}\text{NO} + \text{NO}_2 \leftrightarrow \text{NO} + ^{15}\text{NO}_2$ (Walters and Michalski, 2015; Walters, Simonini, and Michalski (2016). A full description of the relative importance of these effects can be found in Fang et al. (2021). These two hypotheses are not mutually exclusive. Indeed, it is likely to be a combination of both source and chemistry, but their relative importance likely shifts depending on environmental conditions such as a region's NO_x source diversity, plume versus dispersed chemistry, photolysis intensity, and oxidant load. In turn, the $\delta^{15}\text{N}$ data might be a new key to reconciling some of the current

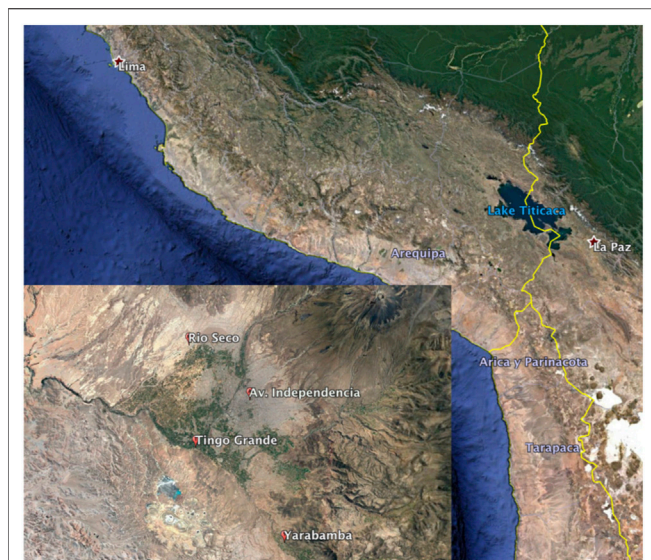


FIGURE 1 | Peru-Chile-Bolivia tri-border with the study area of Arequipa in the inset marking the location of the four sampling locations. The Cerra Verde copper mine can be seen to the south of Tingo Grande and the dormant Andean volcano Misti in the upper right of the inset. Agricultural areas are visible in green on the city edge and the surrounding desert in earth-tone. Image from Google Earth.

uncertainties in NO_x sources and chemistry, if it can be properly interpreted. Isotopic studies of NO_{3atm}⁻ have been primarily conducted in the northern hemisphere and polar regions and relatively few in the subtropical southern hemisphere (Song et al., 2021), particularly in South America. There have been no studies of NO_{3atm}⁻ isotopes in Peru nor in any urban sites in all of South America. The objective of this study is to investigate the source of NO_x and the oxidation chemistry using the N isotope composition of NO_{3atm}⁻ collected in Arequipa, Peru.

METHODS

Study Area

The city of Arequipa (**Figure 1**) is the second most populated city in Peru with a population of ~1 million people located 2,350 m above sea level at 71°32'05" W, 16°23'56" S. Arequipa is an isolated city with the closest major urban centers being Tacna, Peru (Pop. ~280,000) and Arica, Chile (Pop. ~230,000) roughly 250 km to the SE, La Paz, Bolivia (~770,000) 380 km to the east, and Lima located ~800 km to the NW. Therefore, Arequipa's air quality is not significantly impacted by regional anthropogenic N pollution from urban centers outside of the city. It sits at the base on the Andean forearc and at the foot of the active volcano Misti and extinct volcanos Chachani and Pichu. Arequipa is at the northern edge of the hyper-arid Atacama Desert, sometimes called the Sechura Desert in Peru, and the landscape is characterized by wide sandy plains and dunes and sparse vegetation except in a few

river valleys (quebradas) and the Andean highlands. Arequipa's climate is dry throughout the year with annual precipitation averaging ~100 mm that almost exclusively occurs during a rainy season extending from January to March. The weather is mild with daily temperature averages of 15 ± 1.6°C and relative humidity averages of 42 ± 21.5% during the 2019 study year (Weatheronline.co.uk. accessed 2019). The region contributes about 5.6% of the nation's GDP, with mining (23.9%), manufacturing (18.2%), services (17%), commerce (14.6%) and agriculture (12.6%) as the main economic activities (DIGESA, 2005). Agriculture is largely limited to a few river valleys that drain from the Andes, including one that passes through the city, and several large-scale desert irrigation projects (**Figure 1**).

Arequipa PM Collection Sites and Methodology

Sample collection was performed at four sites throughout Arequipa that were located in urban, industrial, suburban, and agricultural sections of the city (**Figure 1**). The urban site Avenida Independencia (AI), is located near the city center where vehicle congestion is very heavy during the week. The industrial site Rio Seco (RS) is located near borate pesticide manufacture plants, tanneries, brick kilns, and chicken processing plants. This district is also located near the main highway by which trucks and buses exit the city and many of the roads in this district are unpaved. Tingo Grande (TG), is a suburban development located in the western edge of the city (2,600 masl) and 6 km due north of a large open pit copper mining operation. Yarabamba (YB), is a small town located 15 km outside of the city center surrounded by rural farmland.

PM_{2.5} samples were collected using a high-volume air sampler (ECOTECH ECO-HVS3000). Sample collection took place periodically throughout the year 2018 by moving the sampler from one sampling site to another. After each relocation, 24 h PM_{2.5} aerosol samples were collected for three consecutive days before the sampler was moved to the next location. There were sampling gaps during the months of April, June, and July due to limited resources such as power outages and labor shortages. The flow rate was ~1 m³/min and total volume as determined as a function of flow rate and time and corrected to standard temperature (273K) and pressure (101.3 kPa). The filter media was either pre-combusted quartz fiber filters (8 in × 10 in, Whatman, United States) or Teflon filters. Since filter sampling often collects both pNO₃⁻ and HNO₃(g) we refer to the samples as NO_{3atm}⁻. Filters were equilibrated to room temperature and relative humidity and the PM mass was determined gravimetrically. The filters were then sectioned into 10 equal width strips used for various chemical, isotopic, and optical analysis. One of the filter sections was soaked in 15 ml of Milli-Q water for 20 min to extract water soluble anions and then filtered (0.45 μm Fisher Scientific, USA) and analyzed for anions, cations and nitrate isotopes.

Geochemical and Isotopic Analysis of Arequipa PM Collection

Nitrate concentrations and nitrogen isotopes were measured using standard techniques. Anion and cation concentrations were determined via standard methods using suppressed ion chromatography (Metrohm 940 Vario Professional). Anion eluent was a carbonate buffer (3.2 mM Na₂CO₃ and 1.0 mM NaHCO₃) and cation eluent was an oxalic acid solution (3.5 mM). The detection limit was 0.01 ppm and the accuracy and precision of the analysis was less than 0.3% and 0.3 ppm, respectively, based on replicate analysis of standard solutions. Nitrogen isotopes of nitrate were measured by converting NO₃⁻ into N₂O using TiCl₃ reduction in 12-ml vials (Altabet et al., 2019). The N₂O was extracted from the vials using a custom-made headspace cryogenic concentrator unit, purified using gas chromatography fitted with a PoraplotQ column. The gas stream is introduced into a Thermo DeltaV isotope ratio mass spectrometer through a custom-made helium flow open split and isotope ratios are determined by measured at Faraday cups tuned to detect ions with masses of 44, 45, and 46 amu. Based on standard replicates and bracketed calibrations curves the accuracy was 0.4‰ and a precision of 0.4‰. Three internal nitrate standards were used that were previously calibrated relative to international standards USGS 32, 34, and 35 (Michalski et al., 2002; Bohlke et al., 2003). Nitrate δ¹⁵N values are reported with respect to air N₂ and are reported in parts per thousand (‰) with a standard error that was 0.3‰ for δ¹⁵N.

Arequipa Meteorology, Trace Gas Data, Chemistry Modeling, and Stable Isotope Approaches

Additional atmospheric data was obtained from the few available datasets in the Arequipa region. Meteorological data (temperature, relative humidity) for the sampling period was acquired from Arequipa's Rodríguez Ballón International Airport (purchased through Weather Online Data Center, <https://www.woeurope.eu/>). Additional wind and air humidity data were obtained from the United States National Oceanic and Atmospheric Administration's (NOAA) Global Data Assimilation System 0.5-degree model. There was very little ancillary trace gas data available for the study period, which highlights the limited air quality research in the region. The local Arequipa Health Ministry monitored PM, CO, SO₂, NO_x, and O₃ during 2010–2011 (Arequipa, G.R. 2020) but these measurements were discontinued thereafter. During the study period there were 8 months of SO₂ monitoring and a few months of PM measurements.

We used *i*_NRACM (Fang et al., 2021), an isotope enabled version of the Regional Atmospheric Chemical Model (RACM), a 0-D photochemical box model (Stockwell et al., 1997) to simulate atmospheric nitrate production. Briefly, the *i*_NRACM traces 17 stable inorganic compounds, four inorganic intermediates, 32 stable organic compounds,

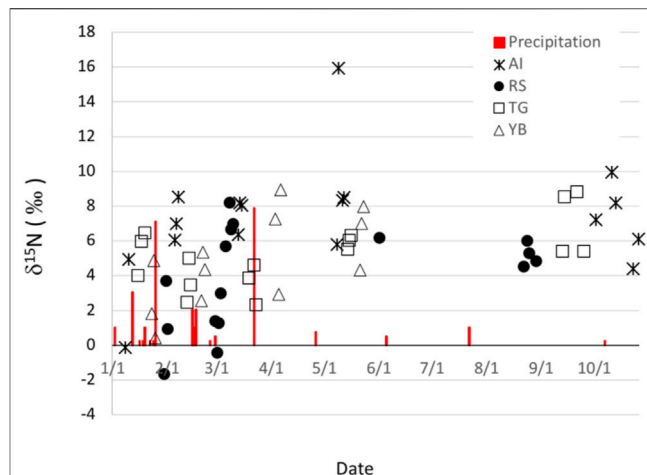


FIGURE 2 | Arequipa PM_{2.5} nitrate δ¹⁵N values at the four sampling sites: Avenida Independencia (AI), Rio Seco (RS) Tingo Grande (TG) and Yarabamba (YB). Precipitation events are in red and are in units of mm. Data gaps in May and June-August were due to resource limitations.

including four biogenic organics, and 24 organic intermediates as they are transformed by 237 chemical reactions, including 23 photolysis reactions (Atkinson, 1990; Atkinson et al., 1992). The *i*_NRACM added ¹⁵N isotopologues for the two primary (NO, NO₂) and the 11 secondary N pollutants found in the original RACM mechanism and rate constants that accounted for relevant isotope effects. *i*_NRACM was also modified to account for heterogeneous N₂O₅ reactions on aerosols that are known to be important for atmospheric nitrate formation. This was done by reducing N₂O₅ heterogeneous hydrolysis to a first order reaction with a rate constant that is a function of N₂O₅ molecular speed, the N₂O₅ uptake coefficient and the aerosol surface area density (Riemer et al., 2003).

*i*_NRACM initial conditions and emissions were based on the limited available data. Temperature, relative humidity (RH), pressure data, and [SO₂] were taken from observations during the study year. Initial CO, O₃, and NO_x were taken from the monthly averages of the 2010–2011 Arequipa Health Ministry data set, under the assumption that the average of these trace gases did not significantly change between 2011 and 2018. This seems justified since the population changed by less than 10% during this time frame. VOC initial concentrations were based on average urban values taken from Stockwell et al. (1997). NO_x and VOC emissions rates were based the equipartition of annual VOC and NO_x emissions from the 2005 DIGESA emission inventory (DIGESA, 2005), the only inventory compiled in the region, and scaled up by 20% based on the population increase between 2005 and 2018. An aerosol mass-surface area ratio of 140 μg/cm² (Guelle et al., 2001) and the observed PM₁₀ mass (Valdivia et al., 2020) was used to determine the aerosol surface area density used in calculating the N₂O₅ uptake coefficient.

RESULTS AND DISCUSSION

Results for PM Nitrate Concentrations and $\delta^{15}\text{N}$ Values

Aerosol nitrate $\delta^{15}\text{N}$ values varied throughout the year and were positive except for two of the samples. The aerosol nitrate $\delta^{15}\text{N}$ values ranged from a minimum of -1.8‰ to a maximum of 16‰ (outlier) and averaged $5.3 \pm 3.0\text{‰}$. There is no obvious seasonal or location dependence of the aerosol nitrate $\delta^{15}\text{N}$ values, but the lower values tended cluster in the southern hemisphere summer months (Jan.–March) when sparse rains occur (Figure 2). The $\delta^{15}\text{N}$ values for the 3 days at any given sampling site tended to be $\pm 2\text{--}3\text{‰}$. Nitrate and other water-soluble ions varied over the course of the year and between sites. PM nitrate concentrations ranged from a minimum of 0.17 mg/m^3 to a maximum of 2.87 mg/m^3 and averaged 0.90 mg/m^3 and accounted for 9–12% of the ion mass. The most abundant anion was SO_4^{2-} (average = $3.1 \pm 1.3\text{ mg/m}^3$) accounting for $\sim 35\%$ of the total ion mass and Cl^- was less than NO_3^- and made up less than 8% of total ion mass. Na^+ and Ca^{2+} were the main cations (SI Supplementary Figures S1, S2), averaging $0.96 \pm 0.38\text{ mg/m}^3$ and $0.87 \pm 0.62\text{ mg/m}^3$ followed by NH_4^+ ($0.57 \pm 0.28\text{ mg/m}^3$).

Comparison of Arequipa PM Nitrate $\delta^{15}\text{N}$ Values With Other Studies

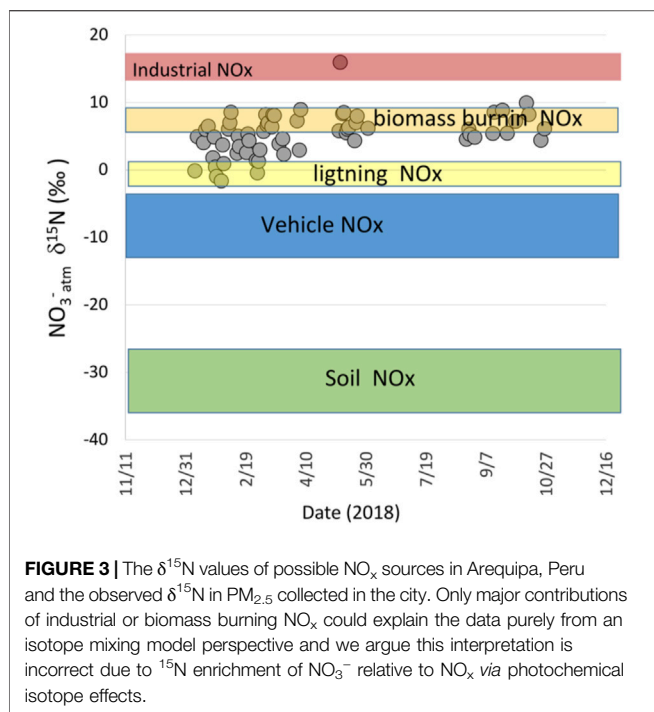
There are only a handful of studies investigating the $\delta^{15}\text{N}$ of NO_3^- collected from the midlatitudes in the southern hemisphere that we can draw on to compare with our data (Song et al., 2021). Most southern hemisphere NO_3^- isotope data have been focused on polar samples from Antarctica (Jarvis et al., 2009; Berhanu et al., 2015; Savarino et al., 2016; Walters et al., 2019) that has unique NO_3^- isotope dynamics due to volatilization and photolysis of HNO_3/NO_x occurring in the snowpack (Jarvis et al., 2009; Berhanu et al., 2015) that makes for a poor comparison for our data. Thus, we focus our comparison on the non-polar, southern hemisphere data. NO_3^- isotopes were determined on aerosols collected along S-N transect across the Atlantic Ocean between Cape Town, South Africa, and northern France during April/May (Morin et al., 2009). Open ocean NO_3^- between 30°S and 10°N had $\delta^{15}\text{N}$ values value were mostly negative (with respect to air N_2), ranging from -7.1 to -1.6‰ , averaging $-4 \pm 2\text{‰}$ and only became positive when influenced by urban/industrial plumes (Morin et al., 2009). In contrast, the Arequipa NO_3^- $\delta^{15}\text{N}$ were almost all positive during the year and in April/May they ranged narrowly between $+4$ and $+8\text{‰}$ (excluding the $+16\text{‰}$ outlier). Measurements of $\delta^{15}\text{N}$ values of NO_3^- collected at a coastal site in New Zealand (Li et al., 2021) were similar to the mid-Atlantic, ranging from -12‰ to $+6\text{‰}$. But most values were negative averaging at -4‰ , and the lowest was April $\delta^{15}\text{N}$ was around -8‰ , significantly lower than those in Arequipa. In addition, in New Zealand, there was a significant seasonal variation, with higher $\delta^{15}\text{N}$ values in the winter (range: -5‰ to $+6\text{‰}$; mean: 0‰) relative to summer

(-12‰ to -4‰ ; -8‰). In contrast, the Arequipa the seasonal effect is less obvious relative to New Zealand, with the summer months (Jan-March) encompassing all of the lowest $\delta^{15}\text{N}$ values. The $\delta^{15}\text{N}$ of NO_3^- collected in dry deposition along a E-W transect in northern Chile were similar to our Arequipa results (Wang et al., 2014). Long-term (2 years) collection of NO_3^- in the Atacama Desert, 800 km south of Arequipa, had $\delta^{15}\text{N}$ values ranging from $+1.5$ to $+10.6\text{‰}$, that generally decreased from $\delta^{15}\text{N}$ highs along the coast ($\sim +8.5\text{‰}$) and Andes ($+10.5\text{‰}$) to central valley values of $+4.0 \pm 2\text{‰}$ (Wang et al., 2014). This average is similar to the annual mean in Arequipa of $+5.3\text{‰}$, suggesting similar NO_x sources and/or photochemical oxidation pathways in both these regions. Along the inland portion of the Chile transect, the $+4.0 \pm 2\text{‰}$ $\delta^{15}\text{N}$ value was attributed to mobile NO_x sources associated with the city of Calama, regional mining vehicles, and the Chilean central highway. Any seasonal variation associated with the transect deposition was masked by the 2-years collection period. These comparisons suggest that southern hemisphere ocean/coastal NO_3^- is either derived from unique NO_x sources relative to southern hemisphere urban environments, like Arequipa, or that possibly the oxidation pathways converting NO_x into NO_3^- are different in cleaner environments relative to urban systems.

Northern hemisphere NO_3^- $\delta^{15}\text{N}$ values tend to be lower than those in Arequipa. Average Northern Hemisphere NO_3^- $\delta^{15}\text{N}$ cluster around $0 \pm 3\text{‰}$ (SI Supplementary Figure S3) with urban values tending to slightly elevated relative to suburban values. East Asia values tend to be higher than North America and Europe, probably due to fewer NO_x reduction systems on coal burning power plants that are prevalent in East Asia. Arequipa's NO_3^- $\delta^{15}\text{N}$ values appear to be generally higher than those in the northern hemisphere where NO_x emissions are significantly higher than in the southern hemisphere.

Arequipa NO_x Source Apportionment Using $\delta^{15}\text{N}$ Mass Balance

In order to try and explain the $\delta^{15}\text{N}$ values of Arequipa NO_3^- , and its variation, we first test the NO_x “source hypothesis” by comparing to the measured NO_3^- $\delta^{15}\text{N}$ values to NO_x sources using an isotope mixing model. The source hypothesis claims that NO_x is converted into NO_3^- relatively quickly and completely, resulting in $\delta^{15}\text{N}$ values of the product NO_3^- identical to the source NO_x . According to a 2004 regional NO_x inventory (DIGESA, 2005), the two main anthropogenic sources of NO_x in Arequipa are vehicles that account for 8,114 tonne $\text{NO}_x\text{ yr}^{-1}$ and industry, contributing 1,072 tonne $\text{NO}_x\text{ yr}^{-1}$ and roughly 80% of this is from coal combustion used during cement production. Arequipa vehicle NO_x is generated primarily (DIGESA, 2005) by old trucks and buses without catalytic converters (70%) and newer automobiles with NO_x reduction controls (30%). The $\delta^{15}\text{N}$ values of vehicle NO_x is mainly determined by whether the vehicle has NO_x reduction technology such as 3-way catalytic converters. Gas and diesel



engines without NO_x reduction technology generate isotopically light NO_x of around -15‰ , due to the KIE of ^{14}N reacting faster than ^{15}N as N_2 fragments in the engine cylinder during combustion (Walters et al., 2015). In contrast, newer vehicles with NO_x reduction catalytic converters tend to produce NO_x of around -2‰ (Walters et al., 2015; Miller et al., 2017) because for the same mechanistic reason, the KIE of ^{14}N reacting faster than ^{15}N as NO_x is reduced by the catalytic converter (for details see Walters et al., 2015). We used a simple two component isotope mixing model to predict the $\delta^{15}\text{N}$ from vehicles ($\delta^{15}\text{N}_{\text{veh}}$).

$$\delta^{15}\text{N}_{\text{veh}} = f_{\text{cat}}\delta^{15}\text{N}_{\text{cat}} + f_{\text{nc}}\delta^{15}\text{N}_{\text{nc}} \quad (2)$$

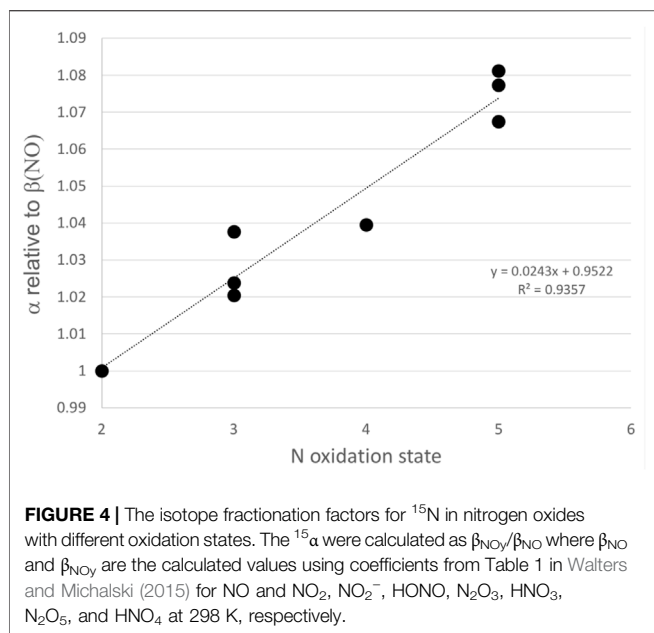
$$f_{\text{nc}} + f_{\text{cat}} = 1 \quad (3)$$

Where f_{cat} and f_{nc} are the molar fractions of NO_x from vehicles with catalytic converters and without, respectively, and $\delta^{15}\text{N}_{\text{cat}}$ and $\delta^{15}\text{N}_{\text{nc}}$ are the $\delta^{15}\text{N}$ values of NO_x emitted by those same vehicles. This yields a vehicle NO_x $\delta^{15}\text{N}$ of approximately -11‰ . Industrial NO_x is primarily from coal burning during cement production and brick kiln operations that lack emission control technology. Previous research has shown that without emission controls, coal burning generates NO_x with a $\delta^{15}\text{N}$ of $\sim +14$ to $+18\text{‰}$ (Felix et al., 2012), similar to the highest $\delta^{15}\text{N}$ value in Arequipa NO_3^- of $+12\text{‰}$. Using another two-component mixing model and assuming industry ($f_{\text{ind}} = 0.12$, $\delta^{15}\text{N} = +16$) and vehicles ($f_{\text{veh}} = 0.88$) are the dominant anthropogenic NO_x sources, isotope mass balance gives an expected anthropogenic NO_x in Arequipa a $\delta^{15}\text{N}$ of -8‰ (Figure 3). This is significantly lower than the Arequipa average ($+5.3\text{‰}$) or even the lowest value (-1.8‰) and would suggest that either industrial (coal burning) NO_x is significantly underestimated, there is an uncounted for NO_x source with high a $^{15}\text{N}/^{14}\text{N}$ ratio, or that chemistry has altered the $\delta^{15}\text{N}$ during the conversion of NO_x into NO_3^- via kinetic, equilibrium, or photolysis isotope effects (Fang et al., 2021).

It is unlikely that the discrepancy between the measured Arequipa NO_3^- $\delta^{15}\text{N}$ and that expected from NO_x source accounting can be resolved by assuming higher industrial emissions. Industrial emissions would need to be more than half of total NO_x emissions to achieve isotope mass balance. Yet coal burning, the main industrial NO_x source in the region, accounts for roughly 10% of total NO_x (DIGESA, 2005) and this is from a single massive modern cement production plant (Yura S.A.) with quantified production rates and emission factors. Thus, industrial NO_x emission uncertainty is low (DIGESA, 2005) and certainly not a factor of five higher than current estimates.

There is also no known natural NO_x source with high a $^{15}\text{N}/^{14}\text{N}$ ratio that could explain the elevated $\delta^{15}\text{N}$ values of NO_3^- in Arequipa. Natural NO_x is almost exclusively from either emission by soils during microbial nitrification and denitrification, produced by lightning, or biomass burning (natural or anthropogenic). None of these has significantly positive $\delta^{15}\text{N}$ values to lead to elevated $\delta^{15}\text{N}$ in PM nitrate. In fact soil NO_x has the lowest $\delta^{15}\text{N}$ (-25‰ to -40‰) of all known NO_x sources (Li & Wang, 2008; Yu & Elliott, 2021). Further, soils are a considered minor source of NO_x southern Peru because of the desert environment, minimal natural vegetation, and low amounts of rainfall. Indeed, a recent high resolution ($0.25^\circ\text{lat.} \times 0.3125^\circ\text{long.}$) global NO_x inventory (Weng et al., 2020) shows that in the Arequipa region less than $72 \times 10^{-5} \text{ TgN yr}^{-1}$ is attributed to soil emissions, less than 10% of the city anthropogenic emissions. Likewise, lightning has low $\delta^{15}\text{N}$ values ($\sim 0\text{‰}$) and is also considered a small source of NO_x in the area. Recent satellite analysis of lightening by Bond et al. (2002) found that while lightening accounted for roughly 23% of NO_x in the tropics, it accounted for less than 1% over Peru west of the Andes including the Arequipa region. Thus, neither lightning nor soil NO_x emissions can explain the positive $\delta^{15}\text{N}$ value of NO_3^- observed in Arequipa.

Biomass burning derived NO_x , either local or transported into the Arequipa region, is potential source, but both its $\delta^{15}\text{N}$ values and other evidence suggest it cannot explain the observed elevated PM $\delta^{15}\text{N}$ values. Biomass burning emissions are due to agricultural practices, forest clearing, and natural fires and the $\delta^{15}\text{N}$ of NO_x derived from biomass burning is nearly identical to the $\delta^{15}\text{N}$ of the foliage being burned (Fibiger & Hastings, 2016). There is some local biomass burning in the Arequipa region used as means of removing crop residues and for pest management (field observations). The $\delta^{15}\text{N}$ of crops are largely reflect a combination of the $\delta^{15}\text{N}$ of the soil in which they grow (Hogberg, 1997) and the $\delta^{15}\text{N}$ of applied fertilizer. Agriculture soil in the Arequipa district have $\delta^{15}\text{N}$ of $\sim 2\text{‰}$ (Filley, personal communication) and inorganic fertilizers are $\sim 0 \pm 2\text{‰}$ (Bateman & Kelly, 2007; Michalski, Kolanowski, & Riha, 2015). This suggests that local biomass burning NO_x $\delta^{15}\text{N}$ values would be just slightly positive and cannot significantly elevate the local NO_x $\delta^{15}\text{N}$. Likewise, large biomass burning events that are seasonal occurrences in the Amazon Basin east of the Andes burn biomass with average $\delta^{15}\text{N}$ of only $+5\text{‰}$ (Ometto et al., 2006). Some of these aerosols are known to be transported over the Andes by advected air masses (Bourgeois et al., 2015) yet the vast majority are removed by deposition and cloud chemistry as they pass



through the planetary boundary layer (PBL) into the free troposphere as they surmount the Andes. After reaching the western side of the Andes they are diluted as they mix across the Pacific over a lifetime of 7–8 days and are quite slow to mix back into the PBL (Bourgeois et al., 2015). Amazon biomass burning occurs predominately in the dry season from June to November (Reddington et al., 2019), but our $\delta^{15}\text{N}$ of PM NO₃⁻ in April–May is not significantly different relative to the biomass burning months of August–November. In addition, biomass burning aerosols are predominately organic carbon and the sum of Cl⁻, NO₃⁻, and NH₄⁺ make up less than 5% of the aerosol mass (Reddington et al., 2019).

Back trajectory analysis and ion data also suggest biomass burning (local or distant) in a minor NO_x source in Arequipa. 48-h HYSPLIT back trajectory ensemble runs show that the origin of most air masses reaching Arequipa are from the ocean (43%) and the northern desert (34%), and only 18% of air masses are derived from the Andean highlands or Amazon (SI Supplementary Figure S4). The $\delta^{15}\text{N}$ of NO_{3atm}⁻ in PM derived from the eastern air masses (8‰) is no different from the average. Potassium cations (K⁺) are a geochemical tracer of biomass burning (Andreae, 1983). PM_{2.5} K⁺ concentrations in Arequipa were $0.42 \pm 0.19 \text{ mg/m}^3$ and were not significantly higher in the biomass burning season (SI Supplementary Figure S2). Further K⁺ is best correlated with Na⁺ ($R^2 = 0.45$) suggesting dust derived from local desert surface is the main K⁺ source (Olson et al., 2021; Li et al., 2021). We conclude that based on the small positive $\delta^{15}\text{N}$ value of biomass NO_x, the limited transport from biomass burning regions, and the lack of significant potassium variations that biomass burn can be considered a negligible NO_x source and cannot account for the elevated $\delta^{15}\text{N}$ values of NO_{3atm}⁻ observed throughout the year in Arequipa. Thus, the $\delta^{15}\text{N}$ of Arequipa NO_{3atm}⁻ is difficult

to reconcile from the perspective of NO_x sources controlling the $\delta^{15}\text{N}$ values.

A two NO_{3atm}⁻ source mixture to explain elevated values (or the annual $\delta^{15}\text{N}$ variation) is also not supported by an isotope Keeling plot. In a two source system, regressing $\delta^{15}\text{N}$ values versus $1/[\text{NO}_3^- \text{N}]$ should yield a correlation with a γ -intercept that defines the $\delta^{15}\text{N}$ of one of the sources, in this case an unknown source(s) with elevated $\delta^{15}\text{N}$ (Keeling, 1961). The Keeling plot for Arequipa $\delta^{15}\text{N}$ vs. $1/[\text{NO}_3^-]$ showed no correlation with an R^2 of 0.07. This indicates that there is not an unknown ¹⁵N enriched NO_x source (or combination of enriched sources) mixing with the combined known local NO_x sources. These considerations suggest that the elevated $\delta^{15}\text{N}$ of NO_{3atm}⁻ in Arequipa PM_{2.5} is due, in part, to kinetic, equilibrium, and photolysis isotope effects occurring during the oxidation of NO_x in NO_{3atm}⁻.

Calculations of isotope equilibrium suggest that during the oxidation of NO_x, NO_y compounds, including NO_{3atm}⁻, should become isotopically enriched relative to the initial NO_x, which qualitatively explains the elevated $\delta^{15}\text{N}$ values for NO_{3atm}⁻ in Arequipa relative to other southern hemisphere locations. At equilibrium, N compounds tend to incorporate ¹⁵N preferentially into molecules with stronger bonds, which is usually a function of the compound's oxidation state. For example, calculated isotope fractionation factors (¹⁵α) of nitrogen oxides at 298 K (Walters and Michalski, 2015) increase (relative to NO) as the N oxidation state increases (Figure 4) from 2 (NO) to 5 (HNO₃, N₂O₅, and HNO₄). Here, the isotope enrichment is defined as $\delta^{15}\text{N} = (\alpha - 1) \times 1,000$. The result would be the $\delta^{15}\text{N}$ of NO_{3atm}⁻ would be elevated relative to the emission source, leaving behind NO_x with lower $\delta^{15}\text{N}$ that could be transported away from the source area. This isotope photochemistry effect would explain elevated NO_{3atm}⁻ $\delta^{15}\text{N}$ values near emission sources (Arequipa) and low NO_{3atm}⁻ $\delta^{15}\text{N}$ values in remote ocean regions (Morin et al., 2009; Li et al., 2021) since it would form from the residual NO_x transported from the continents. This is analogous to water vapor isotopes becoming depleted as a function of the rainout fraction and

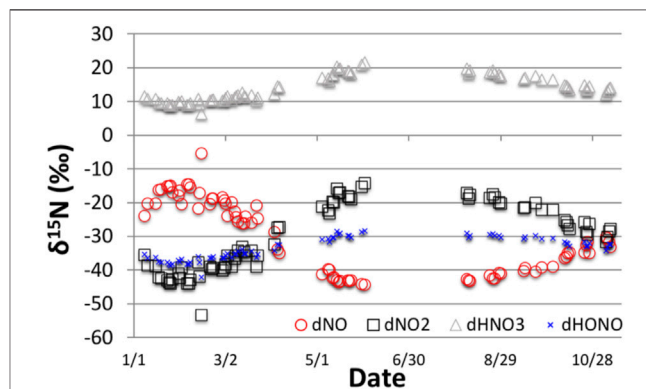
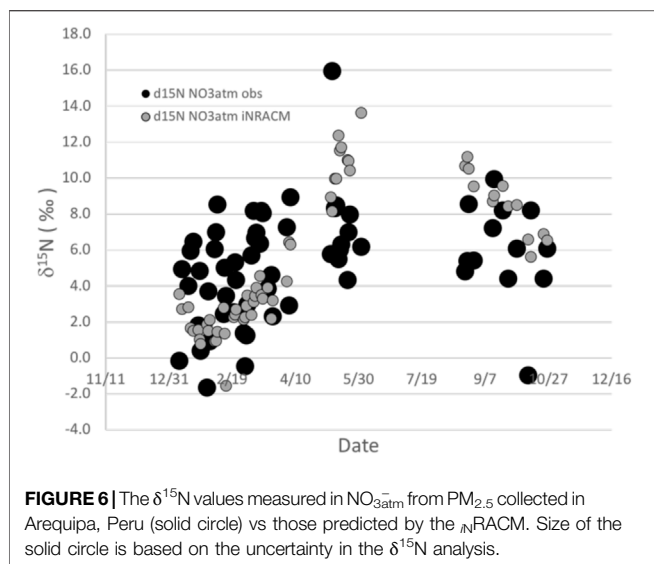


FIGURE 5 | The $\delta^{15}\text{N}$ values of NO₃⁻ (HNO₃), NO, NO₂ and HONO predicted by _NRACM for Arequipa conditions for a NO_x defined as 0‰. $\delta^{15}\text{N}$ shifts between NO and NO₂ is due to NO–NO₂ isotope exchange (Walters et al., 2016). The enrichment of NO_{3atm}⁻ is due kinetic, equilibrium and photolysis isotope effects as discussed in Fang et al., 2021)



depositing isotopically light rain as a function of distance or altitude (Gat, 1996).

Quantifying the Influence of Photochemical Isotope Effects on Nitrate $\text{PM} \delta^{15}\text{N}$ Using $i\text{N-RACM}$

We quantitatively explored the photochemistry effect in Arequipa using the isotope enabled $i\text{N-RACM}$ photochemical box model (Fang et al., 2021). Briefly, the model accounts for kinetic isotope effects associated with bimolecular reactions such as $\text{NO} + \text{O}_3 \rightarrow \text{NO}_2 + \text{O}_2$ (Walters and Michalski (2016), equilibrium isotope effects such as NO_x isotope exchange (Walters et al., 2016), and photolysis isotope effects, mainly $\text{NO}_2 \rightarrow \text{NO} + \text{O}$ (Fang et al., 2021). In addition, the model accounts for the amount of NO_x converted to nitrate, and has demonstrated that when conversion reaches 100%, the $\text{NO}_{3\text{atm}}^- \delta^{15}\text{N}$ is the same as the NO_x source but that isotope fractionation is greatest when conversion fractions are small, similar to more simplistic Rayleigh models. The $i\text{N-RACM}$ model predicts that the $\text{NO}_{3\text{atm}}^- \delta^{15}\text{N}$ values are elevated by 10–20‰ relative to the NO_x source, while the residual NO_x becomes ^{15}N depleted (Figure 5). There is a seasonality to the $\delta^{15}\text{N}$ values, with the southern hemisphere late fall months (May) having higher values and the Summer/Spring months with lower values (Figure 5). This is driven primarily by differences in daylight hours and thus the isotope sensitivity of photolysis reactions. When the initial NO_x source is shifted to -8‰, based on our isotope mass balance mixing model of known NO_x sources (discussion above) the $i\text{N-RACM}$ model does a fair job of replicating the data (Figure 6). For example, the spread in $\text{NO}_{3\text{atm}}^- \delta^{15}\text{N}$ values observed in the May and Aug–Oct. ($\pm 3\%$) is captured by the $i\text{N-RACM}$ model though the modeled values in May are shifted upward by about six‰ relative to the observed values. The $i\text{N-RACM}$ model tends to under predict the observed $\delta^{15}\text{N}$ values during the summer months (Jan–Mar.), nor does it capture the roughly $\pm 4\%$ spread in the values during this period. The root mean square error (RMSE) between the model and data assuming a 0‰ source is 8.9‰, but and improves to

3.7‰ when the source is assumed to be -8‰ based on our isotope mass balance mixing model (Figure 3). The accuracy of the $i\text{N-RACM}$ model on a day-by-day comparison is less robust, with a model versus observed $R^2 = 0.14$.

The inability of the $i\text{N-RACM}$ model to accurately predict the day by day $\text{NO}_{3\text{atm}}^- \delta^{15}\text{N}$ values is not surprising given the assumptions in the model. The main limitation of the $i\text{N-RACM}$ model is the assumption that the daily NO_x source mixture $\delta^{15}\text{N}$ is single valued. This is clearly not the case when considering the main NO_x source, based on the local emission inventory, of vehicle NO_x . We defined the NO_x from vehicles without catalyzed NO_x reduction technologies as a single value (-15‰), when in fact this is only an average and that individual vehicles can range from -7‰ to -19‰. This range believed to be caused is by kinetic isotope effects occurring in the Zeldovich mechanism during fuel combustion in the engine cylinder (Walters et al., 2015). The kinetics and subsequent isotope effect is thus a function of the engine efficiency and running conditions. Likewise, NO_x from vehicles with catalyzed NO_x reduction technology also exhibit a significant range (-19‰ to +10‰). This is caused by the NO_x reduction efficiency of the catalytic converter which in turn is a function of the converter temperature and drive time, with the $\text{NO}_x \delta^{15}\text{N}$ values becoming less negative and even going positive as NO_x reduction is maximized (Walters et al., 2015). Likewise, other known NO_x sources (industry, biomass burning) and natural sources (soil, lightning) are temporally variable. Thus, some of the $\pm 3\%$ spread in the observed $\delta^{15}\text{N}$ values not captured by the $i\text{N-RACM}$ model could simply be due to variations in NO_x sources with time. Regular and reliable trace gas monitoring (NO_x , O_3 , CO) in Arequipa would help resolve this uncertainty in future studies.

Another limitation of the $i\text{N-RACM}$ model's ability to accurately predict the day by day $\text{NO}_{3\text{atm}}^- \delta^{15}\text{N}$ values is that it neither accounts for atmospheric transport nor $\text{NO}_{3\text{atm}}^-$ removal. Atmospheric transport is important in that the PM sampled may have derived from outside the city and transported in or under low wind conditions be primarily of city origin. If there were a clear difference between non-urban and urban $\text{NO}_{3\text{atm}}^- \delta^{15}\text{N}$ values, then this difference should be evident in the Keeling isotope plot (Figure 4) if the two sources are well mixed, which it is not. However, transport cannot be conclusively ruled out. Deposition of $\text{NO}_{3\text{atm}}^-$ is important because it minimizes (maximizes) what can be viewed as an isotope steady state. For example, under stagnant winds and dry conditions urban NO_x would be emitted and converted into $\text{NO}_{3\text{atm}}^-$ and the longer those conditions prevail the closer the $\delta^{15}\text{N}$ value of $\text{NO}_{3\text{atm}}^-$ would be to those of the emitted NO_x via isotope mass balance, which is the steady state condition (Fang et al., 2021). In contrast, after a rainstorm that removes most $\text{NO}_{3\text{atm}}^-$ by wet deposition, the system will reset and the $\delta^{15}\text{N}$ value of $\text{NO}_{3\text{atm}}^-$ would become a function of not only the $\text{NO}_x \delta^{15}\text{N}$ but also the isotope effects that occur during the initial partitioning into the NO_y reservoirs (Fang et al., 2021). This may partially explain the greater range of $\delta^{15}\text{N}$ values during the rainy season. In other words, the relative importance of the “source” versus “chemistry” isotope effects is a function of $\text{NO}_{3\text{atm}}^-$ residence time. Since neither transport nor removal are in the $i\text{N-RACM}$ model it cannot capture this

residence time effect. A more accurate modeling system would be a 3-D chemical transport model that incorporates both temporal/spatial NO_x emission rates and their δ¹⁵N values, 3-D mixing via pressure/temperature gradients, and N isotope effects incorporated into its chemical mechanism. Unfortunately, such a model does not yet exist.

CONCLUSION

We report on the first time series of δ¹⁵N in aerosol nitrate (PM_{2.5}) from South America. PM_{2.5} was collected at four sites located in Arequipa, a major city in southern Peru. PM_{2.5} nitrate concentrations ranged from a minimum of 0.17 mg/m³ to a maximum of 2.87 mg/m³ and averaged 0.90 mg/m³ and accounted for 9–12% of the ion mass. Nitrate δ¹⁵N values ranged from −1.7–15.9‰ and averaged 5.3 ± 3.0‰, with no significant difference between the four study sites and no discernable seasonal trend, but this lack of a seasonal trend may be an artifact of gaps in the data and the movement of the sampler between the sampler over the course of a year. These δ¹⁵N values are significantly higher than those in aerosol nitrate from southern hemisphere marine environments and those from the northern hemisphere. An isotope enabled 0-D photochemical box model (*in*RACM; Fang et al., 2021) was used to estimate the isotope enrichment of nitrate relative to NO_x due to kinetic, equilibrium, and photolysis isotope effects occurring during NO_x oxidation. After correcting for the photochemical isotope effect, we estimated a NO_x sources with δ¹⁵N of −8 ± 3‰. Using an isotope mass balance mixing model that utilized known NO_x source δ¹⁵N it was determined that NO_x in Arequipa is derived mainly from anthropogenic sources (vehicles and some industry), in general agreement a recent emission inventory. Without the photochemical isotopes effect correction, the data indicates a NO_x source with a significantly positive δ¹⁵N value, possibly coal burning or biomass burning, which is unlikely given the sparse vegetation in the region. This suggests that the photochemical isotope effect must be accounted for if nitrate δ¹⁵N values are to be used to accurately constrain NO_x sources. If it is accounted, then measurements PM nitrate δ¹⁵N values could be a new tool to validate NO_x emission

inventories in other locations. This is of particular relevance in regions where detailed NO_x emissions inventories are lacking, such as South America and Africa. Further, the “photochemistry + source” hypothesis can be further tested in regions where NO_x sources are more varied and the NO_x inventories are the thought to be more accurate (US, Europe) by measuring PM nitrate δ¹⁵N at high temporal and spatial scales.

DATA AVAILABILITY STATEMENT

The original contributions presented in the study are included in the article/**Supplementary Materials**, further inquiries can be directed to the corresponding author.

AUTHOR CONTRIBUTIONS

GM is the PI, analyzed the data, and wrote the manuscript. AE and JR collected the PM samples and conducted the gravimetric analysis. HF and JL conducted the modeling and isotope analysis. EO prepared the samples for analysis and conducted ion analysis. LW is Co-Pi and assisted in preparing the manuscript and training students.

FUNDING

For this work provided by the Arequipa Nexus Institute for Food, Energy, Water, and the Environment through the Universidad Nacional de San Agustín (UNSA), Arequipa Peru. A cooperation between UNSA and Purdue University, United States of America. Funding was also provided by the Purdue Climate Change Research Center (PCCRC) and the National Science Foundation NSF P2C2 program.

SUPPLEMENTARY MATERIAL

The Supplementary Material for this article can be found online at: <https://www.frontiersin.org/articles/10.3389/fenvs.2022.916738/full#supplementary-material>

REFERENCES

- Altabet, M. A., Wassenaar, L. I., Douence, C., and Roy, R. (2019). A Ti(III) Reduction Method for One-step Conversion of Seawater and Freshwater Nitrate into N₂O for Stable Isotopic Analysis of 15 N/14 N, 18 O/16 O and 17 O/16 O. *Rapid Commun. Mass Spectrom.* 33 (15), 1227–1239. doi:10.1002/rcm.8454
- Álvarez-Tolentino, D., and Suárez-Salas, L. (2020). Aporte Cuantitativo De Las Fuentes De Pm10 Y Pm2.5 En Sitios Urbanos Del Valle Del Mantaro, Perú. *Rica* 36 (4), 875–892. doi:10.20937/rica.53473
- Andreae, M. O., and Crutzen, P. J. (1997). Atmospheric Aerosols: Biogeochemical Sources and Role in Atmospheric Chemistry. *Science* 276 (5315), 1052–1058. doi:10.1126/science.276.5315.1052
- Andreae, M. O. (1983). Soot Carbon and Excess Fine Potassium: Long-Range Transport of Combustion-Derived Aerosols. *Science* 220, 1148–1151. doi:10.1126/science.220.4602.1148
- Arequipa, G. R. de. (2020). *Salud Arequipa*. Retrieved from Available at: <http://www.saludarequipa.gob.pe/unidades-organicas-3/dir-ejec-de-salud-ambiental/ecologia-proteccion-del-ambiente-y-salud-ocupacional/vigilancia-de-la-calidad-del-aire/>.
- Atkinson, R., Baulch, D. L., Cox, R. A., Hampson, R. F., Kerr, J. A., and Troe, J. (1992). Evaluated Kinetic and Photochemical Data for Atmospheric Chemistry: Supplement IV. IUPAC Subcommittee on Gas Kinetic Data Evaluation for Atmospheric Chemistry. *J. Phys. Chem. Reference Data* 21 (6), 1125–1568. doi:10.1063/1.555918
- Atkinson, R. (1990). Gas-phase Tropospheric Chemistry of Organic Compounds: A Review. *Atmos. Environ. Part A. General Top.* 24 (1), 1–41. doi:10.1016/0960-1686(90)90438-s

- Bateman, A. S., and Kelly, S. D. (2007). Fertilizer Nitrogen Isotope Signatures. *Isotopes Environ. Health Stud.* 43 (3), 237–247. doi:10.1080/10256010701550732
- Berhanu, T. A., Savarino, J., Erbland, J., Vicars, W. C., Preunkert, S., Martins, J. F., et al. (2015). Isotopic Effects of Nitrate Photochemistry in Snow: a Field Study at Dome C, Antarctica. *Atmos. Chem. Phys.* 15 (19), 11243–11256. doi:10.5194/acp-15-11243-2015
- Böhlke, J. K., Mroczkowski, S. J., and Coplen, T. B. (2003). Oxygen Isotopes in Nitrate: New Reference Materials for ^{18}O : ^{17}O : ^{16}O Measurements and Observations on Nitrate-Water Equilibration. *Rapid Commun. Mass Spectrom.* 17, 1835–1846. doi:10.1002/rcm.1123
- Bond, D. W., Steiger, S., Zhang, R., Tie, X., and Orville, R. E. (2002). The Importance of NOx Production by Lightning in the Tropics. *Atmos. Environ.* 36 (9), 1509–1519. doi:10.1016/s1352-2310(01)00553-2
- Boon, R. G. J., Alexaki, A., and Becerra, E. H. (2001). The Ilo Clean Air Project: a Local Response to Industrial Pollution Control in Peru. *Environ. Urbanization* 13 (2), 215–232. doi:10.1177/095624780101300217
- Brimblecombe, P., Hara, H., and Houle, D. (2007). *Acid Rain - Deposition to Recovery*. Springer.
- Brown, S. S., Burkholder, J. B., Talukdar, R. K., and Ravishankara, A. R. (2001). Reaction of Hydroxyl Radical with Nitric Acid: Insights into its Mechanism. *J. Phys. Chem. A* 105 (9), 1605–1614. doi:10.1021/jp002394m
- Brown, S. S., Ryerson, T. B., Wollny, A. G., Brock, C. A., Peltier, R., Sullivan, A. P., et al. (2006). Variability in Nocturnal Nitrogen Oxide Processing and its Role in Regional Air Quality. *Science* 311 (5757), 67–70. doi:10.1126/science.1120120
- Bruningfann, C. S., and Kaneene, J. B. (1993). The Effects of Nitrate, Nitrite and N-Nitroso Compounds on Human Health - A Review. *Veterinary Hum. Toxicol.* 35 (6), 521–538.
- Cao, Z., Zhou, X., Ma, Y., Wang, L., Wu, R., Chen, B., et al. (2017). The Concentrations, Formations, Relationships and Modeling of Sulfate, Nitrate and Ammonium (SNA) Aerosols over China. *Aerosol Air Qual. Res.* 17 (1), 84–97. doi:10.4209/aaqr.2016.01.0020
- Carn, S. A., Krueger, A. J., Krotkov, N. A., Yang, K., and Levelt, P. F. (2007). Sulfur Dioxide Emissions from Peruvian Copper Smelters Detected by the Ozone Monitoring Instrument. *Geophys. Res. Lett.* 34 (9). doi:10.1029/2006gl029020
- Chang, W. L., Bhave, P. V., Brown, S. S., Riemer, N., Stutz, J., and Dabdub, D. (2011). Heterogeneous Atmospheric Chemistry, Ambient Measurements, and Model Calculations of N_2O_5 : A Review. *Aerosol Sci. Technol.* 45 (6), 665–695. doi:10.1080/02786826.2010.551672
- Charlson, R. J., Schwartz, S. E., Hales, J. M., Cess, R. D., Coakley, J. A., Hansen, J. E., et al. (1992). Climate Forcing by Anthropogenic Aerosols. *Science* 255 (5043), 423–430. doi:10.1126/science.255.5043.423
- Chen, W. T., Liao, H., and Seinfeld, J. H. (2007). Future Climate Impacts of Direct Radiative Forcing of Anthropogenic Aerosols, Tropospheric Ozone, and Long-Lived Greenhouse Gases. *J. Geophys. Research-Atmospheres* 112 (D14). doi:10.1029/2006jd008051
- Criss, R. E. (1999). *Principles of Stable Isotope Distribution*. New York: Oxford University Press.
- Digesa (2005). *Inventario de emisiones cuenca atmosferica de la ciudad de Arequipa*. Available at: <http://www.digesa.minsa.gob.pe>
- Elliott, E. M., Kendall, C., Boyer, E. W., Burns, D. A., Lear, G. G., Golden, H. E., et al. (2009). Dual Nitrate Isotopes in Dry Deposition: Utility for Partitioning NOx Source Contributions to Landscape Nitrogen Deposition. *J. Geophys. Research-Biogeosciences* 114. doi:10.1029/2008jg000889
- Elliott, E. M., Kendall, C., Wankel, S. D., Burns, D. A., Boyer, E. W., Harlin, K., et al. (2007). Nitrogen Isotopes as Indicators of NOx Source Contributions to Atmospheric Nitrate Deposition across the Midwestern and Northeastern United States. *Environ. Sci. Technol.* 41 (22), 7661–7667. doi:10.1021/es070898t
- Elliott, E. M., Rose, L., and Felix, J. (2007). *New Insights about the Influence of Reactive Nitrogen Deposition on Ecosystem Processes*.
- Felix, J. D., Elliott, E. M., Avery, G. B., Kieber, R. J., Mead, R. N., Willey, J. D., et al. (2015). Isotopic Composition of Nitrate in Sequential Hurricane Irene Precipitation Samples: Implications for Changing NOx Sources. *Atmos. Environ.* 106, 191–195. doi:10.1016/j.atmosenv.2015.01.075
- Felix, J. D., and Elliott, E. M. (2014). Isotopic Composition of Passively Collected Nitrogen Dioxide Emissions: Vehicle, Soil and Livestock Source Signatures. *Atmos. Environ.* 92, 359–366. doi:10.1016/j.atmosenv.2014.04.005
- Felix, J. D., Elliott, E. M., and Shaw, S. L. (2012). Nitrogen Isotopic Composition of Coal-Fired Power Plant NOx: Influence of Emission Controls and Implications for Global Emission Inventories. *Environ. Sci. Technol.* 46 (6), 3528–3535. doi:10.1021/es203355v
- Feng, Y., and Penner, J. E. (2007). Global Modeling of Nitrate and Ammonium: Interaction of Aerosols and Tropospheric Chemistry. *J. Geophys. Research-Atmospheres* 112 (D1). doi:10.1029/2005jd006404
- Fibiger, D. L., and Hastings, M. G. (2016). First Measurements of the Nitrogen Isotopic Composition of NOx from Biomass Burning. *Environ. Sci. Technol.* 50 (21), 11569–11574. doi:10.1021/acs.est.6b03510
- Finlayson-Pitts, B. J., and Pitts, J. N., Jr. (2000). *Chemistry of the Upper and Lower Atmosphere*. San Diego: Academic Press.
- Freyer, H. D., Kley, D., Volz-Thomas, A., and Kobel, K. (1993). On the Interaction of Isotopic Exchange Processes with Photochemical Reactions in Atmospheric Oxides of Nitrogen. *J. Geophys. Res.* 98 (D8), 14791–14796. doi:10.1029/93jd00874
- Freyer, H. D. (1978). Seasonal Trends of NH_4^+ and NO_3^- Nitrogen Isotope Composition in Rain Collected at Jülich, Germany. *Tellus* 30 (1), 83–92. doi:10.3402/tellusa.v30i1.10319
- Galloway, J. N., Aber, J. D., Erisman, J. W., Seitzinger, S. P., Howarth, R. W., Cowling, E. B., et al. (2003). The Nitrogen Cascade. *Bioscience* 53 (4), 341–356. doi:10.1641/0006-3568(2003)053[0341:tnc]2.0.co;2
- Galloway, J. N., Dentener, F. J., Capone, D. G., Boyer, E. W., Howarth, R. W., Seitzinger, S. P., et al. (2004). Nitrogen Cycles: Past, Present, and Future. *Biogeochemistry* 70 (2), 153–226. doi:10.1007/s10533-004-0370-0
- Gat, J. R. (1996). Oxygen and Hydrogen Isotopes in the Hydrologic Cycle. *Annu. Rev. Earth Planet. Sci.* 24, 225–262. doi:10.1146/annurev.earth.24.1.225
- Guelle, W., Schulz, M., Balkanski, Y., and Dentener, F. (2001). Influence of the Source Formulation on Modeling the Atmospheric Global Distribution of Sea Salt Aerosol. *J. Geophys. Res.* 106 (D21), 27509–27524. doi:10.1029/2001jd900249
- Guo, Y., Zhang, J., An, J., Qu, Y., Liu, X., Sun, Y., et al. (2020). Effect of Vertical Parametrization of a Missing Daytime Source of HONO on Concentrations of HONO, O₃ and Secondary Organic Aerosols in Eastern China. *Atmos. Environ.* 226, 117208. doi:10.1016/j.atmosenv.2019.117208
- Hajat, A., Hsia, C., and O'Neill, M. S. (2015). Socioeconomic Disparities and Air Pollution Exposure: a Global Review. *Curr. Envir Health Rpt* 2 (4), 440–450. doi:10.1007/s40572-015-0069-5
- Hall, J. V., Winer, A. M., Kleinman, M. T., Lurmann, F. W., Brajer, V., and Colome, S. D. (1992). Valuing the Health Benefits of Clean Air. *Science* 255, 812–817. doi:10.1126/science.1536006
- Hastings, M. G., Casciotti, K. L., and Elliott, E. M. (2013). Stable Isotopes as Tracers of Anthropogenic Nitrogen Sources, Deposition, and Impacts. *Elements* 9 (5), 339–344. doi:10.2113/gselements.9.5.339
- Hastings, M. G., Sigman, D. M., and Lipschultz, F. (2003). Isotopic Evidence for Source Changes of Nitrate in Rain at Bermuda. *J. Geophys. Research-Atmospheres* 108 (D24). doi:10.1029/2003jd003789
- Heaton, T. H. E. (1987). Ratios of Nitrate and Ammonium in Rain at Pretoria, South Africa. *Atmos. Environ.* (1967) 21 (4), 843–852. doi:10.1016/0004-6981(87)90080-1
- Högberg, P. (1997). Tansley Review No. 95 15 N Natural Abundance in Soil-plant Systems. *New Phytol.* 137 (2), 179–203. doi:10.1046/j.1469-8137.1997.00808.x
- Huamán De La Cruz, A., Bendezu Roca, Y., Suarez-Salas, L., Pomalaya, J., Alvarez Tolentino, D., and Gioda, A. (2019). Chemical Characterization of PM_{2.5} at Rural and Urban Sites Around the Metropolitan Area of Huancayo (Central Andes of Peru). *Atmosphere* 10 (1), 21. doi:10.3390/atmos10010021
- Jarvis, J. C., Hastings, M. G., Steig, E. J., and Kunasek, S. A. (2009). Isotopic Ratios in Gas-phase HNO_3 and Snow Nitrate at Summit, Greenland. *J. Geophys. Res.* 114. doi:10.1029/2009jd012134
- Kastler, J., and Ballschmiter, K. (1998). Bifunctional Alkyl Nitrates. Trace Constituents of the Atmosphere. *Fresenius' J. Anal. Chem.* 360 (7-8), 812–816. doi:10.1007/s002160050815
- Keeling, C. D. (1961). The Concentration and Isotopic Abundances of Carbon Dioxide in Rural and Marine Air. *Geochimica Cosmochimica Acta* 24 (3-4), 277–298. doi:10.1016/0016-7037(61)90023-0
- Lajtha, K., and Jones, J. (2013). Trends in Cation, Nitrogen, Sulfate and Hydrogen Ion Concentrations in Precipitation in the United States and Europe from 1978

- to 2010: a New Look at an Old Problem. *Biogeochemistry* 116 (1-3), 303–334. doi:10.1007/s10533-013-9860-2
- Larrea Valdivia, A. E., Reyes Larico, J. A., Salcedo Peña, J., and Wannaz, E. D. (2020). Health Risk Assessment of Polycyclic Aromatic Hydrocarbons (PAHs) Adsorbed in PM_{2.5} and PM₁₀ in a Region of Arequipa, Peru. *Environ. Sci. Pollut. Res.* 27 (3), 3065–3075. doi:10.1007/s11356-019-07185-5
- Lelieveld, J., Evans, J. S., Fnais, M., Giannadaki, D., and Pozzer, A. (2015). The Contribution of Outdoor Air Pollution Sources to Premature Mortality on a Global Scale. *Nature*, 525(7569), 367, 371–+. doi:10.1038/nature15371
- Li, D., and Wang, X. (2008). Nitrogen Isotopic Signature of Soil-Released Nitric Oxide (NO) after Fertilizer Application. *Atmos. Environ.* 42 (19), 4747–4754. doi:10.1016/j.atmosenv.2008.01.042
- Li, J., Davy, P., Harvey, M., Katzman, T., Mitchell, T., and Michalski, G. (2021). Nitrogen Isotopes in Nitrate Aerosols Collected in the Remote Marine Boundary Layer: Implications for Nitrogen Isotopic Fractionations Among Atmospheric Reactive Nitrogen Species. *Atmos. Environ.* 245, 118028. doi:10.1016/j.atmosenv.2020.118028
- Li, J., Wang, F., Michalski, G., and Wilkins, B. (2019). Atmospheric Deposition across the Atacama Desert, Chile: Compositions, Source Distributions, and Interannual Comparisons. *Chem. Geol.* 525, 435–446. doi:10.1016/j.chemgeo.2019.07.037
- Lynch, J. A., Bowersox, V. C., and Grimm, J. W. (2000). Acid Rain Reduced in Eastern United States. *Environ. Sci. Technol.* 34 (6), 940–949. doi:10.1021/es9901258
- Michalski, G., Kolanowski, M., and Riha, K. M. (2015). Oxygen and Nitrogen Isotopic Composition of Nitrate in Commercial Fertilizers, Nitric Acid, and Reagent Salts. *Isotopes Environ. Health Stud.* 51 (3), 382–391. doi:10.1080/10256016.2015.1054821
- Michalski, G., Savarino, J., Böhlke, J. K., and Thiemens, M. (2002). Determination of the Total Oxygen Isotopic Composition of Nitrate and the Calibration of a $\Delta^{17}\text{O}$ Nitrate Reference Material. *Anal. Chem.* 74 (19), 4989–4993. doi:10.1021/ac0256282
- Miller, C. E., and Yung, Y. L. (2000). Photo-induced Isotopic Fractionation. *J. Geophys. Res.* 105 (D23), 29039–29051. doi:10.1029/2000jd900388
- Miller, D. J., Wojtal, P. K., Clark, S. C., and Hastings, M. G. (2017). Vehicle NO_x Emission Plume Isotopic Signatures: Spatial Variability across the Eastern United States. *J. Geophys. Res. Atmos.* 122, 4698–4717. doi:10.1002/2016JD025877
- Monks, P. S. (2005). Gas-phase Radical Chemistry in the Troposphere. *Chem. Soc. Rev.* 34 (5), 376–395. doi:10.1039/b307982c
- Monks, P. S., Granier, C., Fuzzi, S., Stohl, A., Williams, M. L., Akimoto, H., et al. (2009). Atmospheric Composition Change - Global and Regional Air Quality. *Atmos. Environ.* 43 (33), 5268–5350. doi:10.1016/j.atmosenv.2009.08.021
- Moore, H. (1977). The Isotopic Composition of Ammonia, Nitrogen Dioxide and Nitrate in the Atmosphere. *Atmos. Environ.* (1967) 11 (12), 1239–1243. doi:10.1016/0004-6981(77)90102-0
- Morin, S., Savarino, J., Frey, M. M., Domine, F., Jacobi, H.-W., Kaleschke, L., et al. (2009). Comprehensive Isotopic Composition of Atmospheric Nitrate in the Atlantic Ocean Boundary Layer from 65°S to 79°N. *J. Geophys. Res.* 114, D05303. doi:10.1029/2008jd010696
- Ometto, J. P. H. B., Ehleringer, J. R., Domingues, T. F., Berry, J. A., Ishida, F. Y., Mazzi, E., et al. (2006). The Stable Carbon and Nitrogen Isotopic Composition of Vegetation in Tropical Forests of the Amazon Basin, Brazil. *Biogeochemistry* 79 (1-2), 251–274. doi:10.1007/s10533-006-9008-8
- Pan, Y., Tian, S., Liu, D., Fang, Y., Zhu, X., Gao, M., et al. (2018). Source Apportionment of Aerosol Ammonium in an Ammonia-Rich Atmosphere: An Isotopic Study of Summer Clean and Hazy Days in Urban Beijing. *J. Geophys. Res. Atmos.* 123 (10), 5681–5689. doi:10.1029/2017jd028095
- Pearce, J. L., Rathbun, S. L., Aguilar-Villalobos, M., and Naeher, L. P. (2009). Characterizing the Spatiotemporal Variability of PM_{2.5} in Cusco, Peru Using Kriging with External Drift. *Atmos. Environ.* 43 (12), 2060–2069. doi:10.1016/j.atmosenv.2008.10.060
- Peng, Q., Palm, B. B., Melander, K. E., Lee, B. H., Hall, S. R., Ullmann, K., et al. (2020). HONO Emissions from Western U.S. Wildfires Provide Dominant Radical Source in Fresh Wildfire Smoke. *Environ. Sci. Technol.* 54 (10), 5954–5963. doi:10.1021/acs.est.0c00126
- Pilegaard, K. (2013). Processes Regulating Nitric Oxide Emissions from Soils. *Philos. Trans. R. Soc. Lond B Biol. Sci.* 368 (1621), 20130126. doi:10.1098/rstb.2013.0126
- Prinn, R. G. (2003). The Cleansing Capacity of the Atmosphere. *Annu. Rev. Environ. Resour.* 28, 29–57. doi:10.1146/annurev.energy.28.011503.163425
- Pusede, S. E., Duffey, K. C., Shusterman, A. A., Saleh, A., Laughner, J. L., Wooldridge, P. J., et al. (2016). On the Effectiveness of Nitrogen Oxide Reductions as a Control over Ammonium Nitrate Aerosol. *Atmos. Chem. Phys.* 16 (4), 2575–2596. doi:10.5194/acp-16-2575-2016
- Pye, H. O. T., Chan, A. W. H., Barkley, M. P., and Seinfeld, J. H. (2010). Global Modeling of Organic Aerosol: the Importance of Reactive Nitrogen (NO_x and NO₂) and NO₃. *Atmos. Chem. Phys.* 10 (22), 11261–11276. doi:10.5194/acp-10-11261-2010
- Reddington, C. L., Morgan, W. T., Darbyshire, E., Brito, J., Coe, H., Artaxo, P., et al. (2019). Biomass Burning Aerosol over the Amazon: Analysis of Aircraft, Surface and Satellite Observations Using a Global Aerosol Model. *Atmos. Chem. Phys.* 19 (14), 9125–9152. doi:10.5194/acp-19-9125-2019
- Riemer, N., Vogel, H., Vogel, B., Schell, B., Ackermann, I., Kessler, C., et al. (2003). Impact of the Heterogeneous Hydrolysis of N₂O₅ on Chemistry and Nitrate Aerosol Formation in the Lower Troposphere under Photosmog Conditions. *J. Geophys. Res.* 108 (D4), 4144. doi:10.1029/2002JD002436
- Romer, P. S., Duffey, K. C., Wooldridge, P. J., Allen, H. M., Ayres, B. R., Brown, S. S., et al. (2016). The Lifetime of Nitrogen Oxides in an Isoprene-Dominated Forest. *Atmos. Chem. Phys.* 16 (12), 7623–7637. doi:10.5194/acp-16-7623-2016
- Romero, Y., Chicchon, N., Duarte, F., Noel, J., Ratti, C., and Nyhan, M. (2020). Quantifying and Spatial Disaggregation of Air Pollution Emissions from Ground Transportation in a Developing Country Context: Case Study for the Lima Metropolitan Area in Peru. *Sci. Total Environ.* 698, 134313. doi:10.1016/j.scitotenv.2019.134313
- Romero, Y., Diaz, C., Meldrum, I., Arias Velasquez, R., and Noel, J. (2020). Temporal and Spatial Analysis of Traffic - Related Pollutant under the Influence of the Seasonality and Meteorological Variables over an Urban City in Peru. *Heliyon* 6 (6), e04029. doi:10.1016/j.heliyon.2020.e04029
- Savard, M. M., Cole, A., Smirnov, A., and Vet, R. (2017). $\delta^{15}\text{N}$ Values of Atmospheric N Species Simultaneously Collected Using Sector-Based Samplers Distant from Sources - Isotopic Inheritance and Fractionation. *Atmos. Environ.* 162, 11–22. doi:10.1016/j.atmosenv.2017.05.010
- Savarino, J., Vicars, W. C., Legrand, M., Preunkert, S., Jourdain, B., Frey, M. M., et al. (2016). Oxygen Isotope Mass Balance of Atmospheric Nitrate at Dome C, East Antarctica, during the OPAL Campaign. *Atmos. Chem. Phys.* 16 (4), 2659–2673. doi:10.5194/acp-16-2659-2016
- Seinfeld, J. H., and Pandis, S. N. (1998). *Atmospheric Chemistry and Physics: From Air Pollution to Climate Change*. 1 ed. New York: Wiley.
- Silva, J., Rojas, J., Norabuena, M., Molina, C., Toro, R. A., and Leiva-Guzmán, M. A. (2017). Particulate Matter Levels in a South American Megacity: the Metropolitan Area of Lima-Callao, Peru. *Environ. Monit. Assess.* 189 (12). doi:10.1007/s10661-017-6327-2
- Song, W., Liu, X.-Y., Hu, C.-C., Chen, G.-Y., Liu, X.-J., Walters, W. W., et al. (2021). Important Contributions of Non-fossil Fuel Nitrogen Oxides Emissions. *Nat. Commun.* 12 (1), 243. doi:10.1038/s41467-020-20356-0
- Spak, S. N., and Holloway, T. (2009). Seasonality of Speciated Aerosol Transport over the Great Lakes Region. *J. Geophys. Research-Atmospheres* 114. doi:10.1029/2008jd010598
- Srivastava, R. K., Hall, R. E., Khan, S., Culligan, K., and Lani, B. W. (2005). Nitrogen Oxides Emission Control Options for Coal-Fired Electric Utility Boilers. *J. Air & Waste Manag. Assoc.* 55 (9), 1367–1388. doi:10.1080/10473289.2005.10464736
- Stein, A. F., Draxler, R. R., Rolph, G. D., Stunder, B. J. B., Cohen, M. D., and Ngan, F. (2015). NOAA's HYSPLIT Atmospheric Transport and Dispersion Modeling System. *Bull. Am. Meteorological Soc.* 96 (12), 2059–2077. doi:10.1175/bams-d-14-00110.1
- Walters, W. W., Fang, H., and Michalski, G. (2018). Summertime Diurnal Variations in the Isotopic Composition of Atmospheric Nitrogen Dioxide at a Small Midwestern United States City. *Atmos. Environ.* 179, 1–11. doi:10.1016/j.atmosenv.2018.01.047
- Walters, W. W., Goodwin, S. R., and Michalski, G. (2015). Nitrogen Stable Isotope Composition ($\delta^{15}\text{N}$) of Vehicle-Emitted NO_x. *Environ. Sci. Technol.* 49 (4), 2278–2285. doi:10.1021/es505580v

- Walters, W. W., and Michalski, G. (2016). An Initial Study of Nitrogen and Position-Specific Oxygen Kinetic Isotope Effects in the NO + O₃ Reaction. *J. Chem. Phys.* 145 (22), 224311. doi:10.1063/1.4968562
- Walters, W. W., Michalski, G., Böhlke, J. K., Alexander, B., Savarino, J., and Thiemens, M. H. (2019). Assessing the Seasonal Dynamics of Nitrate and Sulfate Aerosols at the South Pole Utilizing Stable Isotopes. *J. Geophys. Res. Atmos.* 124 (14), 8161–8177. doi:10.1029/2019jd030517
- Walters, W. W., and Michalski, G. (2015). Theoretical Calculation of Nitrogen Isotope Equilibrium Exchange Fractionation Factors for Various NO_x Molecules. *Geochimica Cosmochimica Acta* 164, 284–297. doi:10.1016/j.gca.2015.05.029
- Walters, W. W., Simonini, D. S., and Michalski, G. (2016). Nitrogen Isotope Exchange between NO and NO₂ and its Implications for $\delta^{15}\text{N}$ Variations in Tropospheric NO_x and Atmospheric Nitrate. *Geophys. Res. Lett.* 43, 440–448. doi:10.1002/2015gl066438
- Walters, W. W., Tharp, B. D., Fang, H., Kozak, B. J., and Michalski, G. (2015). Nitrogen Isotope Composition of Thermally Produced NO_x from Various Fossil-Fuel Combustion Sources. *Environ. Sci. Technol.* 49 (19), 11363–11371. doi:10.1021/acs.est.5b02769
- Wang, F., Michalski, G., Seo, J.-h., and Ge, W. (2014). Geochemical, Isotopic, and Mineralogical Constraints on Atmospheric Deposition in the Hyper-Arid Atacama Desert, Chile. *Geochimica Cosmochimica Acta* 135, 29–48. doi:10.1016/j.gca.2014.03.017
- Weng, H., Lin, J., Martin, R., Millet, D. B., Jaeglé, L., Ridley, D., et al. (2020). Global High-Resolution Emissions of Soil NO_x, Sea Salt Aerosols, and Biogenic Volatile Organic Compounds. *Sci. Data* 7 (1). doi:10.1038/s41597-020-0488-5
- Yu, Z., and Elliott, E. M. (2021). Nitrogen Isotopic Fractionations during Nitric Oxide Production in an Agricultural Soil. *Biogeosciences* 18 (3), 805–829. doi:10.5194/bg-18-805-2021
- Zhang, J., Chen, J., Xue, C., Chen, H., Zhang, Q., Liu, X., et al. (2019). Impacts of Six Potential HONO Sources on HO_x Budgets and SOA Formation during a Wintertime Heavy Haze Period in the North China Plain. *Sci. Total Environ.* 681, 110–123. doi:10.1016/j.scitotenv.2019.05.100
- Zhang, Y., Vijayaraghavan, K., Wen, X. Y., Snell, H. E., and Jacobson, M. Z. (2009). Probing into Regional Ozone and Particulate Matter Pollution in the United States: 1. A 1 Year CMAQ Simulation and Evaluation Using Surface and Satellite Data. *J. Geophys. Research-Atmospheres* 114. doi:10.1029/2009jd011898

Conflict of Interest: The authors declare that the research was conducted in the absence of any commercial or financial relationships that could be construed as a potential conflict of interest.

Publisher's Note: All claims expressed in this article are solely those of the authors and do not necessarily represent those of their affiliated organizations, or those of the publisher, the editors and the reviewers. Any product that may be evaluated in this article, or claim that may be made by its manufacturer, is not guaranteed or endorsed by the publisher.

Copyright © 2022 Michalski, E. Larrea Valdivia, Olson, Welp, Fang, Magara-Gomez, Morales Paredes, Reyes Larico and Li. This is an open-access article distributed under the terms of the Creative Commons Attribution License (CC BY). The use, distribution or reproduction in other forums is permitted, provided the original author(s) and the copyright owner(s) are credited and that the original publication in this journal is cited, in accordance with accepted academic practice. No use, distribution or reproduction is permitted which does not comply with these terms.